 CMC, vol.5, no.3, pp.197-211, 2007

A Fin Design Problem in Determining the Optimum Shape of Non-Fourier Spine and Longitudinal Fins

Cheng-Hung Huang[1] **and Hsin-Hsien Wu**[2]

Abstract: The conjugate gradient method (CGM) is applied in an inverse fin design problem in estimating the optimum shapes for the non-Fourier spine and longitudinal fins based on the desired fin efficiency and fin volume at the specified time. One of the advantages in using CGM in the inverse design problem lies in that it can handle problems having a huge number of design parameters easily and converges very fast.
The validity of using CGM in solving the present inverse design problem is justified by performing the numerical experiments. Several test cases involving different design fin efficiency, design fin volume, specified time and relaxation time are considered and examined. Results show that CGM can be utilized successfully in determining the optimum shape of the non-Fourier spine and longitudinal fins.

Nomenclature

$\overline{A}$	cross-section area
Bi_1, Bi_2	Biot number
$\overline{h}_1, \overline{h}_2$	convective heat transfer coefficient
J	functional defined by equation (3)
J'	gradient of functional defined by equation (17)
$\overline{k}$	thermal conductivity
$\overline{L}$	reference length
$\overline{p}$	perimeter of fin
q	actual heat transfer rate through fin
Q	ideal heat transfer rate through fin
$r(x,t_s)$	fin radius for spine fins and fin thickness for longitudinal fins
$\overline{t}$	dimensional time
$\overline{T}$	dimensional temperature
$v(r,t_s)$	estimated fin volume
V	given fin volume
w	fin width

Greeks

β	search step size
γ	conjugate coefficient
$\theta(x,t)$	estimated dimensionless temperature
$\Delta\theta(x,t)$	sensitivity function defined by equation (8)
Ω	computational domain
$\lambda(x,t)$	Lagrange multiplier defined by equation (15)
$\delta(\bullet)$	Dirac delta function
η	estimated fin efficiency
Φ	desired fin efficiency
ε	convergence criteria
$\overline{\tau}$	dimensional relaxation time

Superscript

n	iteration index
$\overline{\ }$	dimensional quantities

1 Introduction

One of the main goals in designing the modern thermal systems is the achievement of more compact and efficient heat exchangers. This requires employing the finned surfaces to the systems to enhance the heat transfer. Finned surfaces have been in use over a long period of time for dissipation of heat by convection or by radiation. Applications for finned surfaces are widely seen in air-conditioning, refrigeration, cryogenics and many cooling systems in industrial. Many works have

[1] Professor and corresponding author. e-mail: chhuang@mail.ncku.edu.tw. Department of Systems and Naval Mechatronic Engineering, National Cheng Kung University, Tainan, Taiwan 701, R.O.C.
[2] Graduate student. Department of Systems and Naval Mechatronic Engineering, National Cheng Kung University, Tainan, Taiwan 701, R.O.C.

been done in improving the design of the fins.

The design criterion of fins is different for various applications, but the primary concern is the fin volume (or weight) and fin efficiency. It is highly desirable to optimize the shape of fins based on these two constraints. The optimum dimensions for fin with the maximum (or desired) fin efficiency must be justified under the condition of fixed volume of the fin.

Numerous studies have been conducted to optimize the dimensions of spine and longitudinal fins of various profiles subject to convection. A review on extended surfaces over six decades is available in the work by Kraus (1988). Aziz (1992) has published a survey article where the optimum dimensions of straight fins, annular fins and spines of different profiles with many numerical examples are included. For pure conducting fins, a criterion for optimum shape was proposed by Schmidt (1926) using the principle of a constant heat flux. Duffin (1959) confirmed later the results by using a variational method. In their studies, the fin profile is calculated as a parabola and has a zero thickness at the outer edge. An optimum shape of purely radiating fin was obtained by Wilkins (1960,1960) for a variety of geometries. For convective and radiative fins, Kern and Kraus (1972) have presented a thorough study of the optimum design of finned surfaces.

Razelos (1983) and Chung (1983) have independently presented the optimum dimensions of convective pin fin with cylindrical, conical, concave parabolic and convex parabolic profiles. Chung and Iyer (1993) used an integral approach to determine the optimum dimensions for rectangular longitudinal fins and cylindrical pin fins. Yeh (1996) used the Lagrange's multiplier method to find the optimum dimensions of longitudinal rectangular and cylindrical pin fins. Recently, Huang and Hsiao (2003) applied the conjugate gradient method (CGM) in an inverse fin design problem to find the optimum shape of the longitudinal and spine fins with constant thermal properties. Later, the non-linear thermal properties were considered in the fin design problem by the same authors (2003).

In all the above references the optimum shape of fins are determined based on either minimum weight or maximum heat transfer rate through fin base or optimum (or desired) fin efficiency for some specified fin volume using Fourier model. The applications for non-Fourier fin design problems are rarely discussed.

With advances in micro-fabrication technology, the micro-heat exchangers are of interest in many engineering applications, such as cooling of electronic chips and cryocoolers using helium II. For such a situation, phenomena with the finite thermal propagation speed might be important for the thermal analysis of the extended surface in the micro-heat exchangers.

Lin (1998) proposed a hybrid application of the Laplace transform and control volume methods in determining the non-Fourier fins performance under periodic thermal conditions. Results show that the effects of the thermal relaxation time on the fin performance are significant for a short time after the initial transient. This is the so-called direct non-Fourier fin problems. It should be noted that the discussions for thermal behaviors for the direct non-Fourier fin problems are still limited in the open literature, not to mention the non-Fourier fin design problems. Therefore, the purpose of this work is to develop a design algorithm using the conjugate gradient method to estimate the optimum shapes of the non-Fourier spine and longitudinal fins.

Various inverse algorithms have been applied to many different engineering practical applications. Hon and Wei (2005) applied an effective meshless and integration-free method for the numerical solution of multidimensional inverse heat conduction problems. Liu (2006) derived the first-order and second-order one-step GPS applied to the estimation of thermophysical properties. Liu et al (2007) constructed a closed-form estimation method for the inverse thermal problems of estimating the spatial-dependent thermophysical parameters.

Moreover, the conjugate gradient algorithm has also been applied successfully in many inverse problems. Chao et al (2001) used the CGM to determine the unknown traction of a cracked elastic body. Huang and Kim (2005) also used

CGM to estimate the time-dependent reaction coefficient in an autocatalytic reaction pathway. Huang and Lo (2006) utilized the CGM in a three-dimensional inverse problem in estimating the internal heat flux of housing for high speed motors.

For the inverse design problem, it has been utilized to determine the optimum shape of cooling passages for turbine blade [Huang and Hsiung, (1999)] and optimum spine and longitudinal fin shapes for Fourier model [Huang and Hsiao, (2003)]. In this paper we addressed the developments of CGM for estimating optimum shapes of the non-Fourier spine and longitudinal fins at some specified times based on optimum (or desired) fin efficiency and desired fin volume. Moreover, the influence of Biot number on the optimum fin shape will also be discussed.

The CGM derives from perturbation principle, and transforms the inverse design problem to the solution of three problems, namely, the direct problem, the sensitivity problem and the adjoint problem. This method will be discussed in detail in the next few sections.

2 The Direct Problem

To illustrate the methodology for developing expressions for use in designing the optimum shape for the non-Fourier spine and longitudinal fins based on the desired fin efficiency and fin volume at the specified time$\overline{t}_s$, we consider the following fin design problem.

The mathematical formulation of this non-Fourier fin problem in dimensional form is given by:

$$\frac{d}{d\overline{x}}\left[\overline{A}(\overline{x},\overline{t}_s)\frac{d\overline{T}}{d\overline{x}}\right]-\frac{\overline{h}_1\overline{p}(\overline{x},\overline{t}_s)}{\overline{k}}(\overline{T}-\overline{T}_\infty)$$
$$-\frac{\overline{\tau}\overline{h}_1\overline{p}(\overline{x},\overline{t}_s)}{\overline{k}}\frac{\partial}{\partial\overline{t}}(\overline{T}-\overline{T}_\infty)$$
$$=\frac{\overline{\rho}\overline{C}\overline{A}(\overline{x},\overline{t}_s)}{\overline{k}}\frac{\partial\overline{T}}{\partial\overline{t}}$$
$$+\frac{\overline{\rho}\overline{C}\overline{\tau}\overline{A}(\overline{x},\overline{t}_s)}{\overline{k}}\frac{\partial^2\overline{T}}{\partial\overline{t}^2};\qquad \text{in } 0<\overline{x}<\overline{L} \quad (1a)$$

$$\overline{T}=\overline{T}_b;\quad \text{at } \overline{x}=0 \quad (1b)$$

$$\overline{k}\frac{d\overline{T}}{d\overline{x}}+\overline{h}_2\overline{T}=\overline{h}_2\overline{T}_\infty;\quad \text{at } \overline{x}=\overline{L} \quad (1c)$$

$$\overline{T}=0;\quad \text{at } \overline{t}=0 \quad (1d)$$

$$\frac{d\overline{T}}{d\overline{t}}=0;\quad \text{at } \overline{t}=0 \quad (1e)$$

here the over bar "‾" represents dimensional quantities.

$\overline{A}(\overline{x},\overline{t}_s)$ and $\overline{p}(\overline{x},\overline{t}_s)$ represent the cross-section area and perimeter of fin at the specified time $\overline{t}_s$; $\overline{k},\overline{\rho}$ and $\overline{C}$ are the thermal conductivity, density and heat capacity of fin, respectively, and $\overline{\tau}$ is the relaxation time. $\overline{T}_b$ and $\overline{T}_\infty$ are the fin base temperatures at $\overline{x}=0$ and ambient temperature, respectively. $\overline{h}_1$ and $\overline{h}_2$ are the heat transfer coefficients on fin surface and fin tip $\overline{x}=\overline{L}$, respectively. For spine fins $\overline{A}(\overline{x},\overline{t}_s)=\pi\overline{r}(\overline{x},\overline{t}_s)^2$ and $\overline{p}(\overline{x},\overline{t}_s)=2\pi\overline{r}(\overline{x},\overline{t}_s)$, and $\overline{r}(\overline{x},\overline{t}_s)$ represents fin radius. For longitudinal fins $\overline{A}(\overline{x},\overline{t}_s)=\overline{r}(\overline{x},\overline{t}_s)\times\overline{w}$ and $\overline{p}(\overline{x},\overline{t}_s)\approx 2\overline{w}$ (assuming $\overline{r}(\overline{x},\overline{t}_s)<<\overline{w}$), and $\overline{r}(\overline{x},\overline{t}_s)$ represents fin thickness. Here $\overline{w}$ is the width of longitudinal fins.

If the following dimensionless quantities are defined

$$\theta=\frac{\overline{T}-\overline{T}_\infty}{\overline{T}_b-\overline{T}_\infty};\quad x=\frac{\overline{x}}{\overline{L}};\qquad r=\frac{\overline{r}}{\overline{L}};$$
$$Bi_1=\frac{\overline{h}_1\overline{L}}{\overline{k}};\qquad Bi_2=\frac{\overline{h}_2\overline{L}}{\overline{k}};\quad w=\frac{\overline{w}}{\overline{L}};$$
$$t=\frac{\overline{k}\overline{t}}{\overline{\rho}\overline{C}\overline{L}^2};\qquad \tau=\frac{\overline{k}\overline{\tau}}{\overline{\rho}\overline{C}\overline{L}^2}$$

The dimensionless non-Fourier fin equation can be obtained as

$$\frac{\partial}{\partial x}[F_1(x,t_s)\frac{\partial\theta(x,t)}{\partial x}]-2F_2(x,t_s)B_{i1}\theta$$
$$=F_3(x,t_s)\frac{\partial\theta}{\partial t}+F_4(x,t_s)\frac{\partial^2\theta}{\partial t^2} \quad (2a)$$

$$\theta=1;\quad \text{at } x=0 \quad (2b)$$

$$\frac{d\theta}{dx}+Bi_2\theta=0;\quad \text{at } x=1 \quad (2c)$$

$$\theta=0;\quad \text{at } t=0 \quad (2d)$$

$$\frac{\partial\theta}{\partial t}=0;\quad \text{at } t=0 \quad (2e)$$

For spine fins: $F_1(x,t_s)=r(x,t_s)^2$, $F_2(x,t_s)=r(x,t_s)$, $F_3(x,t_s)=r(x,t_s)^2+2Bi_1\tau r(x,t_s)$ and $F_4(x,t_s)=\tau r(x,t_s)^2$ For longitudinal fins: $F_1(x,t_s)=r(x,t_s)$, $F_2(x,t_s)=1.0$,

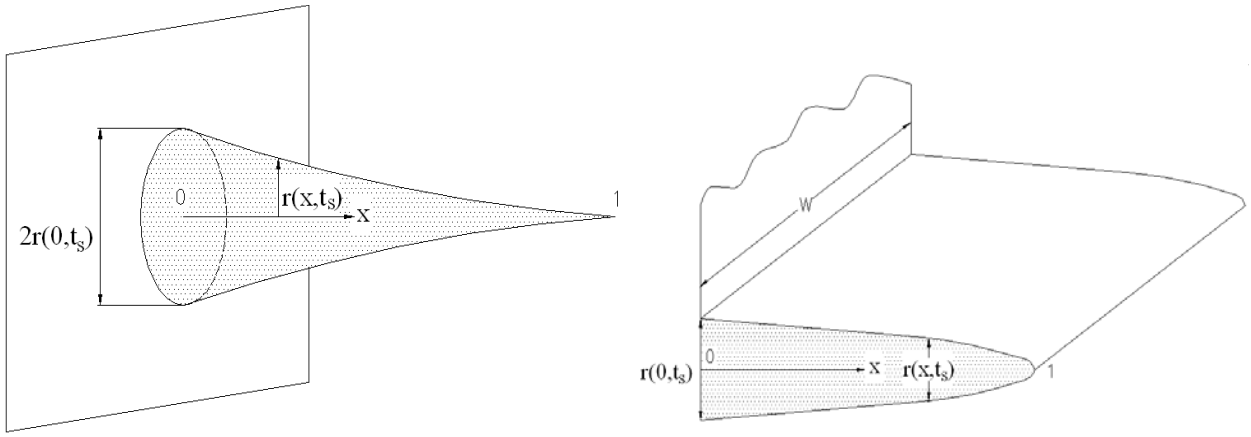

(a) (b)

Figure 1: The (a) spine fin and (b) longitudinal fin.

$F_3(x,t_s) = r(x,t_s) + 2Bi_1\tau$ and $F_4(x,t_s) = \tau r(x,t_s)$. Figures 1a and 1b illustrate the dimensionless geometry for the spine and longitudinal fins considered here.

The direct problem considered here is concerned with the determination of the temperature distribution of non-Fourier fin and its efficiency at the specified time t_s when the shape of fin and the boundary conditions at both boundaries are known and given.

3 The Inverse Design Problem

For the inverse design problem, the shape of fin, i.e. $r(x,t_s)$, is regarded as being unknown, but everything else in equation (2) is known. In addition, desired fin efficiency at the specified time and desired fin volume are given.

The solution of the present inverse design problem is to be obtained in such a way that the following functional is minimized:

$$J(r,t_s) = [q(r,t_s) - \Phi Q(r,t_s)]^2 + \alpha[v(r,t_s) - V]^2 \tag{3}$$

Where $q(r,t_s)$ and $Q(r,t_s)$ are the actual (or estimated) and ideal heat transfer rate of fin at the specified time t_s, respectively. $v(r,t_s)$ and V represent the estimated and desired (or given) fin volume. Φ is the desired fin efficiency and α is the weighting coefficient.

The first and second terms on the right hand side are the square of the deviation between the actual and desired heat transfer rate through fin and the deviation between the estimated and desired fin volume, respectively.

If the value of functional $J(r,t_s)$ is less than the specified stopping criterion ε, stop the iterative process and the optimal shape of fins is obtained, otherwise, continue the iteration until the stopping criterion is satisfied.

Here $q = \frac{\overline{q}}{\overline{q}_{ref}}$, $Q = \frac{\overline{Q}}{\overline{q}_{ref}}$ and $v = \frac{\overline{v}}{\overline{v}_{ref}}$ are defined and the reference quantities are given as

$$\overline{q}_{ref} = \overline{h}_1 \overline{L}^2 (\overline{T}_b - \overline{T}_\infty) \tag{4a}$$

$$\overline{v}_{ref} = \overline{L}^3 \tag{4b}$$

For spine fins we have

$$\overline{q}(\overline{r},\overline{t}_s) = \int_{\overline{x}=0}^{\overline{L}} \overline{h}_1 [2\pi\overline{r}(\overline{x},\overline{t}_s)][\overline{T}(\overline{r},\overline{t}_s) - \overline{T}_\infty] d\overline{x} \tag{5a}$$

$$\overline{Q}(\overline{r},\overline{t}_s) = \int_{\overline{x}=0}^{\overline{L}} \overline{h}_1 [2\pi\overline{r}(\overline{x},\overline{t}_s)](\overline{T}_b - \overline{T}_\infty) d\overline{x} \tag{5b}$$

$$\overline{v} = \int_{\overline{x}=0}^{\overline{L}} \pi\overline{r}(\overline{x},\overline{t}_s)^2 d\overline{x} \tag{5c}$$

thus the dimensionless quantities for q, Q and v can be obtained as

$$q = \int_{t=0}^{t_f} \int_{x=0}^{1} 2\pi r(x,t)\theta(x,t)\delta(t-t_s) dx dt \tag{5d}$$

$$Q = \int_{t=0}^{t_f} \int_{x=0}^{1} 2\pi r(x,t)\delta(t-t_s)dxdt \tag{5e}$$

$$v = \int_{t=0}^{t_f} \int_{x=0}^{1} \pi r(x,t)^2\delta(t-t_s)dxdt \tag{5f}$$

For longitudinal fins, we assumed $\overline{r}(\overline{x},\overline{t}_s) << \overline{w}$ and obtained

$$\overline{q} = \int_{\overline{x}=0}^{\overline{L}} \overline{h}_1(2\overline{w})[\overline{T}(\overline{x},\overline{t}_s) - \overline{T}_\infty]d\overline{x} \tag{6a}$$

$$\overline{Q} = \int_{\overline{x}=0}^{\overline{L}} \overline{h}_1(2\overline{w})[\overline{T}_b(0,\overline{t}_s) - \overline{T}_\infty]d\overline{x} \tag{6b}$$

$$\overline{v} = \int_{\overline{x}=0}^{\overline{L}} \overline{wr}(\overline{x},\overline{t}_s)d\overline{x} \tag{6c}$$

so the dimensionless quantities for q, Q and v can be expressed as

$$q = \int_{t=0}^{t_f} \int_{x=0}^{1} 2w\theta(x,t)\delta(t-t_s)dxdt \tag{6d}$$

$$Q = \int_{t=0}^{t_f} \int_{x=0}^{1} 2w\delta(t-t_s)dxdt \tag{6e}$$

$$v = \int_{t=0}^{t_f} \int_{x=0}^{1} wr(x)\delta(t-t_s)dxdt \tag{6f}$$

The inverse design problem for non-Fourier fins can now be stated as follows: by utilizing the above mentioned functional $J[r(x,t_s)]$, estimate the optimum shape of the fins, i.e. $r(x,t_s)$, such that the actual (or estimated) heat transfer rate of fin q approaches to Φ, Q and the estimated fin volume v approaches to the desired fin volume V at the specified time t_s.

The conjugate gradient method has the ability in optimizing the above non-Fourier fin design problem and will be discussed in detail in the next few sections.

4 Conjugate Gradient Method for Minimization

The following iterative process based on CGM [Alifanov, (1994)] is now used for the estimation of the unknown fin shape $r(x,t_s)$ by minimizing the functional $J[r(x,t_s)]$.

$$r^{n+1}(x,t_s) = r^n(x,t_s) - \beta^n P^n(x,t_s) \tag{7a}$$

Here β^n is the search step size in going from iteration n to iteration $n+1$ and $P^n(x,t_s)$ is the direction of descent (i.e. search direction) given by

$$P^n(x,t_s) = J'^n(x,t_s) + \gamma^n P^{n-1}(x,t_s) \tag{7b}$$

which is a conjugation of the gradient in the outward normal direction $J'^n(x,t_s)$ at iteration n and the direction of descent $P^{n-1}(x,t_s)$ at iteration $n-1$. The conjugate coefficient is defined as [Alifanov, (1994)]:

$$\gamma^n = \frac{\int_{x=0}^{1} \left(J'^n\right)^2 dx}{\int_{x=0}^{1} \left(J'^{n-1}\right)^2 dx}; \quad \text{with } \gamma^0 = 0 \tag{7c}$$

It is noted that when $\gamma^n = 0$ for any n, the direction of descent $P^n(x,t_s)$ becomes the gradient direction in equation (7b), i.e. the Steepest Descent Method (SDM) is obtained. The convergence of the above iterative procedure in minimizing the functional J is guaranteed in [Lasdon et al, (1967)].

To perform the iterations according to equation (7a), a step size β^n and the gradient of the functional $J'^n(x,t_s)$ need to be computed. In order to develop expressions for the determination of these two quantities, a "sensitivity problem" and an "adjoint problem" are constructed as described below.

5 Sensitivity Problem and Search Step Size

The sensitivity problem is obtained from the original direct problem defined by equation (2) in the following manner: It is assumed that when $r(x,t_s)$ undergoes a variation $\Delta r(x,t_s)$, $\theta(x,t_s)$ is perturbed by $\Delta\theta(x,t_s)$. Then replacing in the direct problem $r(x,t_s)$ by $r(x,t_s)+\Delta r(x,t_s)$ and $\theta(x,t_s)$ by $\theta(x,t_s)+\Delta\theta(x,t_s)$, subtracting the resulting

expressions from the direct problem and neglecting the second-order terms, the following sensitivity problem for the sensitivity function $\Delta\theta(x,t_s)$ is obtained.

$$\frac{\partial}{\partial x}\left[F_5(x,t_s)\frac{\partial \Delta\theta}{\partial x}\right]+\frac{\partial}{\partial x}\left[F_6(x,t_s)\frac{\partial \theta}{\partial x}\right] = 2B_{i1}[F_7(x,t_s)\Delta\theta+F_8(x,t_s)\theta]+F_9(x,t_s)\frac{\partial \theta}{\partial t} + F_{10}(x,t_s)\frac{\partial \Delta\theta}{\partial t}+F_{11}(x,t_s)\frac{\partial^2\theta}{\partial t^2}+F_{12}(x,t_s)\frac{\partial^2\Delta\theta}{\partial t^2} \quad (8a)$$

$$\Delta\theta = 0; \quad \text{at } x=0 \quad (8b)$$

$$\frac{d\Delta\theta}{dx}+Bi_2\Delta\theta = 0; \quad \text{at } x=1 \quad (8c)$$

$$\Delta\theta = 0; \quad \text{at } t=0 \quad (8d)$$

$$\frac{\partial\Delta\theta}{\partial t} = 0; \quad \text{at } t=0 \quad (8e)$$

For spine fins: $F_5(x,t_s)=r(x,t_s)^2$, $F_6(x,t_s)=2r(x,t_s)\Delta r(x,t_s)$, $F_7(x,t_s)=r(x,t_s)$, $F_8(x,t_s)=\Delta r(x,t_s)$, $F_9(x,t_s)=2\tau Bi_1\Delta r(x,t_s)+2r(x,t_s)\Delta r(x,t_s)$, $F_{10}(x,t_s)=r(x,t_s)^2+2Bi_1\tau r(x,t_s)$, $F_{11}(x,t_s)=2\tau r(x,t_s)\Delta r(x,t_s)$ and $F_{12}(x,t_s)=\tau r(x,t_s)^2$. For longitudinal fins: $F_5(x,t_s)=r(x,t_s)$, $F_6(x,t_s)=\Delta r(x,t_s)$, $F_7(x,t_s)=x$, $F_8(x,t_s)=w$, $F_9(x,t_s)=\Delta r(x,t_s)$, $F_{10}(x,t_s)=r(x,t_s)+2Bi_1\tau$, $F_{11}(x,t_s)=\tau\Delta r(x,t_s)$ and $F_{12}(x,t_s)=\tau r(x,t_s)$.

The functional $J(r^{n+1},t_s)$ for iteration $n+1$ is obtained by rewriting equation (3) as

$$J(r^{n+1},t_s)=[q(r^n-\beta^n p^n,t_s)-\Phi Q(r^n-\beta^n p^n,t_s)]^2 + \alpha[v(r^n-\beta^n p^n,t_s)-V]^2 \quad (9a)$$

where we replaced r^{n+1} by the expression given by equation (7a). If the terms $q(r^n-\beta^n p^n,t_s)$, $Q(r^n-\beta^n p^n,t_s)$ and $v(r^n-\beta^n p^n,t_s)$ are linearized by a Taylor expansion, equation (9a) takes the form

$$J(r^{n+1},t_s) = \{q(r^n,t_s)-\beta^n[\Delta q(p^n,t_s)-\Phi\Delta Q(p^n,t_s)] - \Phi Q(r^n,t_s)\}^2+\alpha[v(r^n,t_s)-\beta^n\Delta v(p^n,t_s)-V]^2 \quad (9b)$$

Here the expressions for Δq, ΔQ and Δv can be obtained by using $\Delta q = q(r+\Delta r,t_s)-q(r,t_s)$, $\Delta Q = Q(r+\Delta r,t_s)-Q(r,t_s)$ and $\Delta v = v(r+\Delta r,t_s)-v(r,t_s)$ and neglecting the high order terms. Eventually, for spine fins we have

$$\Delta q=\int_{t=0}^{t_f}\int_{x=0}^{1} 2\pi\left(r\Delta\theta+\theta\Delta r\right)\delta(t-t_s)dxdt \quad (10a)$$

$$\Delta Q=\int_{t=0}^{t_f}\int_{x=0}^{1} 2\pi\Delta r\delta(t-t_s)dxdt \quad (10b)$$

$$\Delta v=\int_{t=0}^{t_f}\int_{x=0}^{1} 2\pi r\Delta r\delta(t-t_s)dxdt \quad (10c)$$

for longitudinal fins we have

$$\Delta q=\int_{t=0}^{t_f}\int_{x=0}^{1} 2w\Delta\theta\delta(t-t_s)dxdt \quad (11a)$$

$$\Delta Q = 0 \quad (11b)$$

$$\Delta v=\int_{t=0}^{t_f}\int_{x=0}^{1} w\Delta r\delta(t-t_s)dxdt \quad (11c)$$

The sensitivity function $\Delta\theta(x,t)$ is taken as the solutions of problem (8) by letting $\Delta r = P^n$. Once $\Delta\theta(x,t)$ is obtained, the above quantities can all be calculated.

The search step size β^n is determined by minimizing the functional given by equation (9b) with respect to β^n. The following expression results:

$$\beta^n=\frac{(q-\Phi Q)(\Delta q-\Phi\Delta Q)+\alpha(v-V)\Delta v}{(\Delta q-\Phi\Delta Q)^2+\alpha\Delta v^2} \quad (12)$$

6 Adjoint Problem and Gradient Equation

To obtain the adjoint problem, equation (2a) is multiplied by the Lagrange multiplier (or adjoint function) $\lambda(x,t)$ and the resulting expression is integrated over the correspondent space domain. Then the result is added to the right hand side of equation (3) to yield the following expression for

the functional $J[r(x,t_s)]$:

$$J(r,t_s) = (q-\Phi Q)^2 + \alpha\,(v-V)^2 + \int_{t=0}^{t_f}\int_{x=0}^{1} \lambda\,(x,t)\left\{\frac{\partial}{\partial x}\left[F_1(x,t_s)\frac{\partial\theta(x,t)}{\partial x}\right] - 2F_2(x,t_s)Bi_1\theta - F_3(x,t_s)\frac{\partial\theta}{\partial t} - F_4(x,t_s)\frac{\partial^2\theta}{\partial t^2}\right\}dxdt \quad (13)$$

The variation ΔJ is obtained by perturbing r by $r+\Delta r$, θ by $\theta+\Delta\theta$, q by $q+\Delta q$, Q by $Q+\Delta Q$ and v by $v+\Delta v$ in equation (13), subtracting the resulting expression from the original equation (13) and neglecting the second-order terms. We thus find

$$\Delta J = 2\,(q-\Phi Q)\,(\Delta q-\Phi\Delta Q) + \alpha\,[2\,(v-V)\,\Delta v] + \int_{t=0}^{t_f}\int_{x=0}^{1}\left\{\lambda\,(x,t)\frac{\partial}{\partial x}\left[F_5(x,t_s)\frac{\partial\Delta\theta}{\partial x}\right] + \frac{\partial}{\partial x}\left[F_6(x,t_s)\frac{\partial\theta}{\partial x}\right] - 2B_{i1}\left[F_7(x,t_s)\Delta\theta + F_8(x,t_s)\theta\right] - F_9(x,t_s)\frac{\partial\theta}{\partial t} - F_{10}(x,t_s)\frac{\partial\Delta\theta}{\partial t} - F_{11}(x,t_s)\frac{\partial^2\theta}{\partial t^2} - F_{12}(x,t_s)\frac{\partial^2\Delta\theta}{\partial t^2}\right\}dxdt \quad (14)$$

In equation (14), the integral terms are reformulated based on the integration by parts; the boundary conditions of the sensitivity problem given by equations (8b) and (8c) are utilized and then ΔJ is allowed to go to zero. The vanishing of the integrands containing $\Delta\theta$ leads to the following adjoint problem for determining $\lambda\,(x,t)$:

$$\frac{\partial}{\partial x}[F_{13}(x,t_s)\frac{\partial\lambda}{\partial x}] + 4(q-\Phi Q)F_{14}(x,t_s) = 2B_{i1}\lambda F_{15}(x,t_s) + F_{16}(x,t_s)\frac{\partial\lambda}{\partial t} + F_{17}\frac{\partial^2\lambda}{\partial t^2} \quad (15a)$$

$$\lambda = 0; \quad \text{at } x = 0 \quad (15b)$$

$$\frac{d\lambda}{dx} + Bi_2\lambda = 0; \quad \text{at } x = 1 \quad (15c)$$

$$\lambda = 0; \quad \text{at } t = 0 \quad (15d)$$

$$\frac{d\lambda}{dt} = 0; \quad \text{at } t = 0 \quad (15e)$$

where $F_{13}(x,t_s) = r(x,t_s)^2$, $F_{14}(x,t_s) = \pi r(x,t_s)$, $F_{15}(x,t_s) = r(x,t_s)$, $F_{16}(x,t_s) = -r(x,t_s)^2 - 2Bi_1\tau r(x,t_s)$ and $F_{17}(x,t_s) = \tau r(x,t_s)^2$ for spine fins and $F_{13}(x,t_s) = r(x,t_s)$, $F_{14}(x,t_s) = w$, $F_{15}(x,t_s) = 1$, $F_{16}(x,t_s) = -r(x,t_s) - 2Bi_1\tau$ and $F_{17}(x,t_s) = \tau r(x,t_s)$ for longitudinal fins.

Finally, the following integral term is left for spine fins

$$\Delta J = \int_{t=0}^{t_f}\int_{x=0}^{1}\left\{2\pi\left[2(q-\Phi Q)(\theta-\Phi) + 2\alpha r(v-V)\right] - 2\lambda Bi_1\theta + 2r\lambda\frac{d\theta}{dx}\delta\,(x-1) - 2r\frac{d\theta}{dx}\frac{d\lambda}{dx} - (2r+2\tau Bi_1)\lambda\frac{\partial\theta}{\partial t} - 2\tau\lambda r\frac{\partial^2\theta}{\partial t^2}\right\}\Delta r dxt \quad (16a)$$

and the following integral term is left for longitudinal fins

$$\Delta J = \int_{t=0}^{t_f}\int_{x=0}^{1}\left\{2\alpha w(v-V) - \lambda\frac{\partial\theta}{\partial t} - \lambda\tau\frac{\partial^2\theta}{\partial t^2} + \lambda\frac{d\theta}{dx}\delta\,(x-1) - \frac{d\theta}{dx}\frac{d\lambda}{dx}\right\}\Delta r dtdx \quad (16b)$$

Where $\delta(\bullet)$ is the Dirac delta function. From definition [Alifanov, (1994)], the functional increment can be presented as

$$\Delta J = \int_{x=0}^{1} J'\Delta r dx \quad (16c)$$

A comparison of equations (16a), (16b) and (16c) leads to the following expression for the gradient $J'(x)$ of the functional $J[r(x)]$ for spine and longi-

tudinal fins, respectively:

$$J'(x) = \int_{t=0}^{t_f} \Big\{ 2\pi \left[2(q-\Phi Q)(\theta-\Phi) + 2\alpha r(v-V) \right] - 2\lambda Bi_1 \theta + 2r\lambda \frac{d\theta}{dx}\delta(x-1) - 2r\frac{d\theta}{dx}\frac{d\lambda}{dx} - (2r+2\tau Bi_1)\lambda\frac{\partial\theta}{\partial t} - 2\tau\lambda r\frac{\partial^2\theta}{\partial t^2} \Big\} dt \quad (17a)$$

and

$$J'(x) = \int_{t=0}^{t_f} \Big\{ 2\alpha w(v-V) - \lambda\frac{\partial\theta}{\partial t} - \lambda\tau\frac{\partial^2\theta}{\partial t^2} + \lambda\frac{d\theta}{dx}\delta(x-1) - \frac{d\theta}{dx}\frac{d\lambda}{dx} \Big\} dt \quad (17b)$$

The calculation of gradient equations is the most important part of CGM since it plays a significant role of the inverse calculation.

7 Computational Procedure

The computational procedure for the solution of this inverse design problem for non-Fourier fins using CGM may be summarized as follows:

Suppose $r^n(x,t_s)$ is available at iteration n.

Step 1. Solve the direct problem given by equation (2) for $\theta(x,t)$.

Step 2. Examine the stopping criterion ε. Continue if not satisfied.

Step 3. Solve the adjoint problem given by equation (15) for $\lambda(x,t)$.

Step 4. Compute the gradient of the functional J'^n from equation (17).

Step 5. Compute the conjugate coefficient γ^n and direction of descent P^n from equations (7c) and (7b), respectively.

Step 6. Set $\Delta r(x,t_s) = P^n(x,t_s)$, and solve the sensitivity problem given by equation (8) for $\Delta\theta(x)$. Then Δq, ΔQ and Δv can be calculated.

Step 7. Compute the search step size β^n from equation (12).

Step 8. Compute the new estimation for $r^{n+1}(x,t_s)$ from equation (7a) and return to step 1.

8 Results and Discussions

The objective of this work is to apply the present inverse design algorithm, i.e. the conjugate gradient method (CGM), in estimating the optimum shapes for the non-Fourier spine and longitudinal fins based on the desired fin efficiency and fin volume at the specified time. No prior information on the functional form of the unknown shapes is given, thus it is also called the function estimation [Beck et al, (1985)].

One should note that the initial guess of the fin shape is always necessary for the present iterative algorithm. To make it more convenient to be applied, we always assume that, for a fixed fin volume, the initial shapes for the spine and longitudinal fin design problems are the pin fin and rectangular fin, respectively.

To illustrate the ability of this inverse design algorithm in estimating the optimum shape for non-Fourier fins from the knowledge of the desired fin efficiency and volume at the specified time, the following two types of problems are considered, i.e. (I). The non-Fourier spine fin design problems and (II). The non-Fourier longitudinal fin design problems.

(I). The Non-Fourier Spine Fin Design Problems:

First, the optimum shape of non-Fourier spine fins is examined by considering perfect fin efficiency, i.e. $\Phi = 1.0$ and using $\Delta x = 0.05$, $\Delta t = 0.1$, $Bi_2 = 0$, $t_s = 200$, $Bi_1 = 1$, 3 and 5, respectively, for a smaller and a larger relaxation time, say τ = 1 and 100, respectively. The desired fin volume is given in the range from $V = 0.002$ to $V = 0.005$ with an increment of 0.0005. It is impossible to obtain the shape of spine fin having $\Phi = 1.0$ under this consideration, however, the optimum fin shape can still be obtained with best fin efficiency.

When the value of weighting coefficient α is small, the constraint for fin volume is loose which means the estimated fin volume may have discrepancy with the desired one. At the same time, the product of β^n and P^n (i.e. the corrected value of fin radius) becomes larger, this also implies that the rate of convergent will be faster. To compromise with both requirements, the value of α is chosen as 10000 at the beginning and is increased gradually during the iterative process.

By performing the above stated inverse design algorithm, the optimum shape of non-Fourier spine fin for various desired fin volumes can be obtained. The value of objection function J can not be decreased to a small number since the desired efficiency $\Phi = 1.0$ can not be satisfied. The stopping criterion under this consideration is used as the follows: if $(J^n - J^{n-1}) < 10^{-10}$, stop the iterative process.

Figures 2a and 2b illustrate the optimum fin efficiency for the estimated spine fin for $\tau = 1$ and 100, respectively. From Figures 2a and 2b we learned that for same desired fin volume, the efficiency of the optimum fin with a smaller relaxation time (higher thermal propagation speed) is always higher than that with a larger relaxation time (lower thermal propagation speed). This is due to the fact that when the relaxation time is larger heat will need more time to travel within the fin, therefore the surface temperature is lower than that for higher relaxation and the fin efficiency becomes lower.

It is also of interest to examine the influence of Biot number Bi_1 on the estimated optimum fin efficiency and fin shape. Figures 2a and 2b also indicate the optimum fin efficiency for various desired fin volumes when Bi_1 is increased from 1 to 3 and then to 5 with $Bi_2 = 0$. From these Figures we noticed that as Bi_1 increases, the optimum fin efficiency η also increases. For a fin with fin shape fixed, when Bi_1 is increased fin surface temperature will be decreased; as a result, the fin efficiency will also be decreased. However, in the present case, the fin shape can be adjusted automatically by the present algorithm to obtain optimum shape that matches best with the constraints. Therefore, it is possible that the fin efficiency increases even when Biot number increases [Huang and Hsiao, (2003)].

Figures 3a and 3b illustrate the optimum fin shapes at $\tau = 100$ and $t_s = 200$ for $Bi_1 = 1$, 3 and 5, respectively, for fin volume $V = 0.003$ and 0.005, respectively. We have learned from these Figures that as Bi_1 increases, fin base radius $r(0,t_s)$ also increases but the rest of fin radius $r(x,t_s)$ decreases to obtain higher fin surface temperature and thus to obtain higher fin efficiency.

Next the present design algorithm is examined by assigning desired fin efficiency and fin volume at different specified time, then estimate the optimum fin shape corresponding to these situations. The desired fin efficiency is always less than the optimum efficiency, we thus expect that the value of the objection function J can be decreased to a small number, so the stopping criterion under this consideration is taken as $\varepsilon = 10^{-8}$. The estimated optimum fin shapes are presented in Figures 4a and 4b for $t_s = 3$ and 20, respectively. It is found that at the same desired fin efficiency and relaxation time, the base area of fin for smaller t_s is bigger than that for larger t_s. This is because that when the specified time is shorter, less heat is entered into the fin than the case of longer specified time due to the characteristic of finite thermal propagation speed. In order to allow more heat enters into the fin to satisfy with the desired fin efficiency, the base area must be increased to allow more heat to enter into the fin.

Figures 5a and 5b show the fin shapes for different relaxation time $\tau = 1$ and 100, respectively, with desired fin efficiency $\Phi = 0.8$ and $t_s = 20$. It is found that under the condition of same fin volume, the base area of fin for larger relaxation time is always bigger than that for smaller relaxation time. It is clear that larger relaxation time represents lower thermal propagation speed. To match with the condition of desired fin efficiency, more heat must enter into the fin. This can only be done by increasing the base area and that is why the base area of fin for a larger relaxation time is always bigger than that for a smaller relaxation time.

Figures 6a and 6b indicate the fin shapes for different specified time $t_s = 3$, 8 and 200, respec-

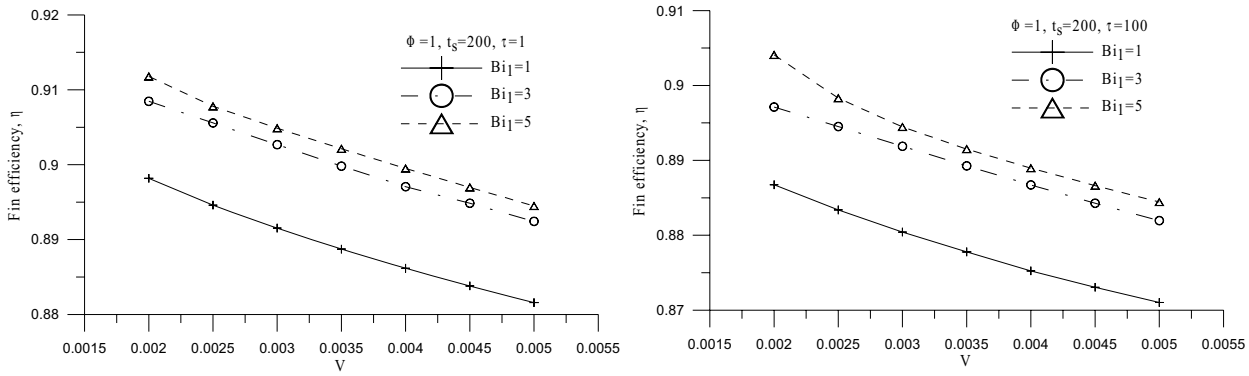

(a) (b)

Figure 2: The optimum fin efficiency for spine fin at $t_s = 200$ by varying Bi_1 for (a) $\tau = 1$ and (b) $\tau = 100$

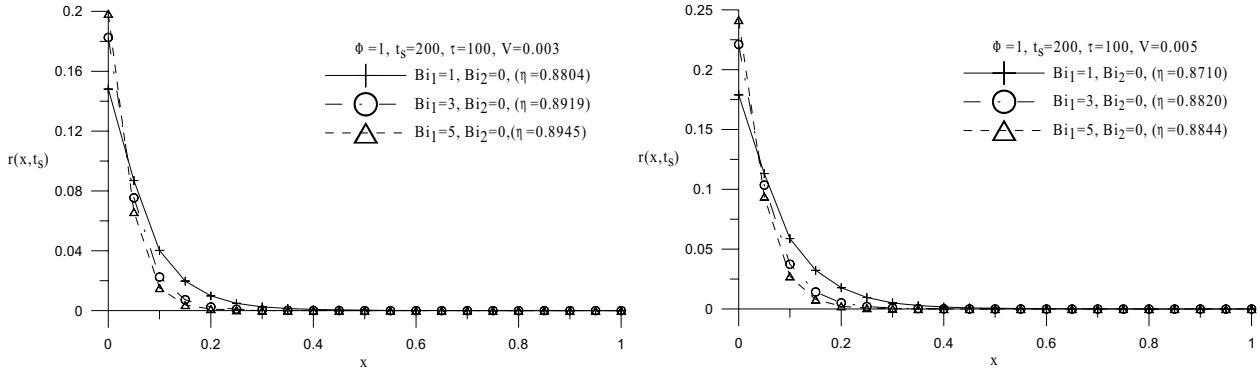

(a) (b)

Figure 3: The optimum spine fin shapes at $t_s = 200$,$\tau = 100$ and (a) $V = 0.003$ and (b) $V = 0.005$

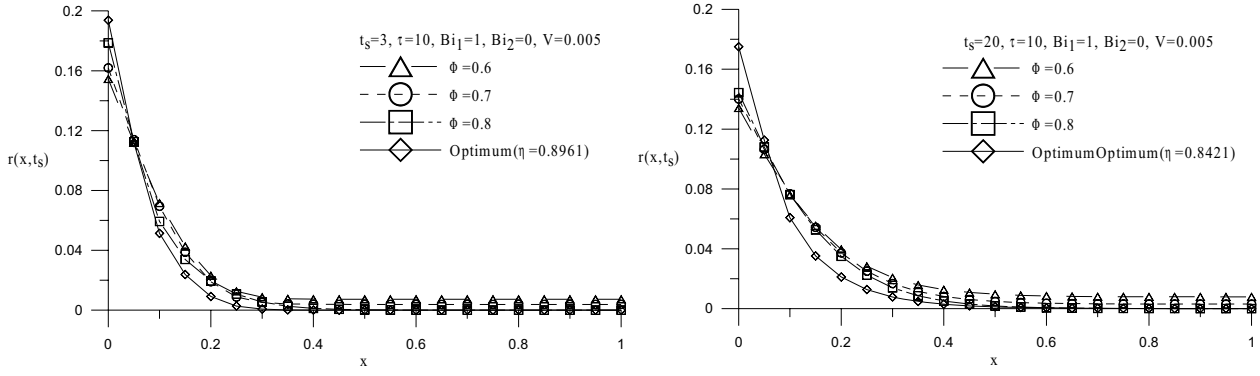

(a) (b)

Figure 4: The optimum spine fin shapes at $\tau = 10$ by varying desired fin efficiency and (a) $t_s = 3$ and (b) $t_s = 20$

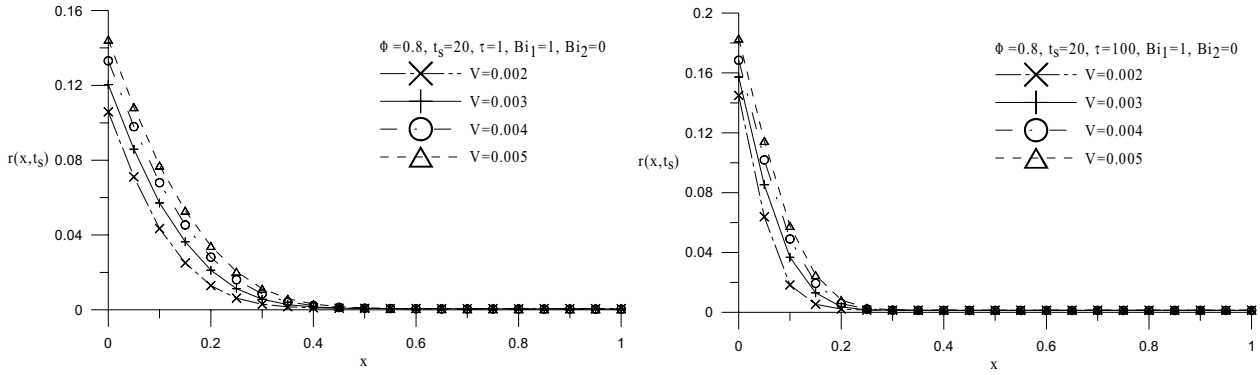

(a) (b)

Figure 5: The optimum spine fin shapes at $\Phi = 0.8$ and $t_s = 20$ by varying desired fin volume and (a) $\tau = 1$ and (b) $\tau = 100$

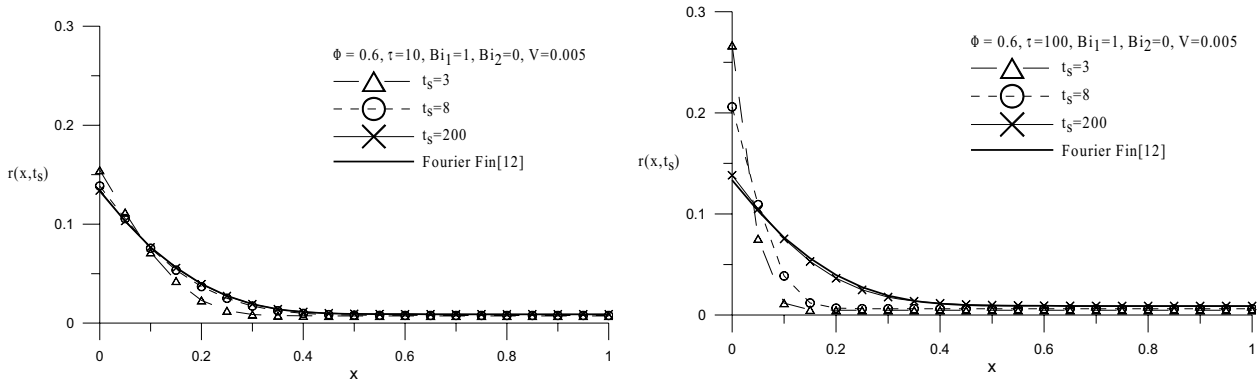

(a) (b)

Figure 6: The optimum spine fin shapes at $\Phi = 0.6$ and $V = 0.005$ by varying t_s and (a) $\tau = 10$ and (b) $\tau = 100$

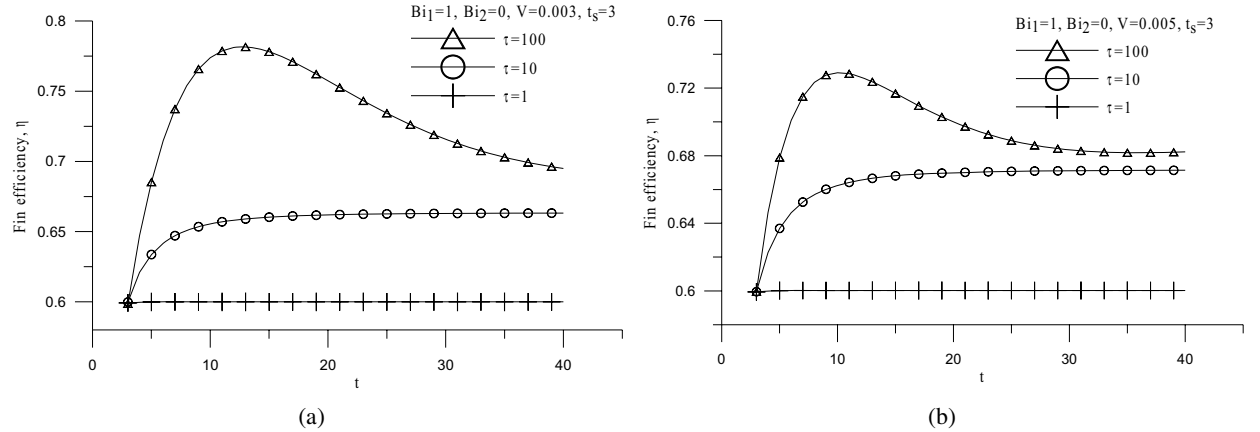

(a) (b)

Figure 7: The optimum spine fin efficiency with time at $t_s = 3$ by varying relaxation time τ and (a) $V = 0.003$ and (b) $V = 0.005$

tively, with desired fin efficiency $\Phi = 0.8$ and $V = 0.005$ for $\tau = 10$ and 100, respectively. It can be seen from Figures 6a and 6b that the base fin area for $\tau = 100$ is always bigger than that for $\tau = 10$ for the reason stated previously. Moreover, it is also found that the optimum non-Fourier fin profile for a smaller relaxation time is easier to approach to the profile of Fourier fin. As the specified time is long enough, the temperature distribution for fin will become steady-state and thus the fin profile is identical to the Fourier fin profile.

Finally it is interesting to examine the fin efficiency with time based on the optimum fin shape with desired fin efficiency $\Phi = 0.6$ obtained at the specified time $t_s = 3$. Figures 7a and 7b show a comparison of the fin efficiency with time at different relaxation time and fin volume. It is clear that for the case $\tau = 1$, the fin reaches steady-state condition at $t_s = 3$ and thus the fin efficiency remains the same with time. However, for $\tau = 10$ and 100, the fin is still in a transient-state at $t_s = 3$ and the fin efficiency varies with time but will reach to a steady-state condition eventually. The fin efficiencies beyond $t_s = 3$ are all better than or equal to the efficiency at $t_s = 3$. This implies that the fin efficiency for the optimum fin is always the same as or better than the efficiency at $t_s = 3$ and therefore the overall fin performance is better than the design value.

(II). The Non-Fourier Longitudinal Fin Design Problems:

The optimum shape of non-Fourier longitudinal fins is first examined by considering perfect fin efficiency, i.e. $\Phi = 1.0$ and using $V = 0.006$, $\Delta x = 0.05$, $\Delta t = 0.1$, $Bi_2 = 0$, $t_s = 3$, $Bi_1 = 1$ and 5 for $\tau = 0.1$, 1 and 10, respectively. The width of fin w is assumed as unity. It is impossible to obtain the optimum shape of non-Fourier longitudinal fin having $\Phi = 1.0$, but the fin shape can still be obtained with best fin efficiency. The value of α is chosen as 10000 at the beginning and is increased gradually during the iterative process as was mentioned previously.

The value of objection function J can not be decreased to a small number for the case $\Phi = 1.0$, therefore the iterative process is stopped when $(J^n - J^{n-1}) < 10^{-7}$. When the above stated inverse design algorithm is performed, the optimum shape of non-Fourier longitudinal fin for various desired fin volumes can be obtained. Figures 8a and 8b indicate the estimated non-Fourier longitudinal fin by varying τ or $Bi_1 = 1$ and 5, respectively.

From Figures 8a and 8b we learned that the efficiency of the optimum non-Fourier longitudinal fin is very low. This is because that the fin width w is fixed and we can adjust only the fin thickness $r(x)$ to optimize the fin efficiency. However, the fin thickness has much less weight than fin width in calculating the total fin surface. For this reason the optimum fin shape can improve only slightly the fin efficiency.

It is observed that when the relaxation time is larger, the fin base area is also bigger. The reason for this is the same for the spine fin and is stated previously. Moreover, it is also observed that at the same relaxation time, when Bi_1 becomes larger, the fin base area becomes also bigger. This is because that when the Biot number is increased the surface temperatures are decreased and thus the fin efficiency is decreased. In order to keep fin efficiency optimum, the fin base area must be increased to let more heat enters into the fin and to increase the surface temperature of the fin and to result in higher fin efficiency.

Figures 9a and 9b show the fin shapes for different specified time $t_s = 3$, 8 and 200, respectively, with desired fin efficiency $\Phi = 0.1$ and V = 0.012 for $\tau = 1$ and 10, respectively. It can be seen from those Figures that the base fin area for $\tau = 10$ is always bigger than that for $\tau = 1$ for the reason stated before. Moreover, it is also found that the optimum non-Fourier fin profile for $\tau = 1$ approaches to the profile of Fourier fin at $t_s = 3$, 8 and 200. This implies that when $\tau = 1$, the fin system has become steady-state for $t_s = 3$, 8 and 200 and the non-Fourier assumption no longer exists and the fin becomes a steady-state Fourier fin. As the relaxation time becomes longer, say $\tau = 10$, the temperature distributions at $t_s = 3$ and 8 are still in a transient-state, therefore the fin shapes differ from the Fourier fin profile. However fin temperature will become steady-state as

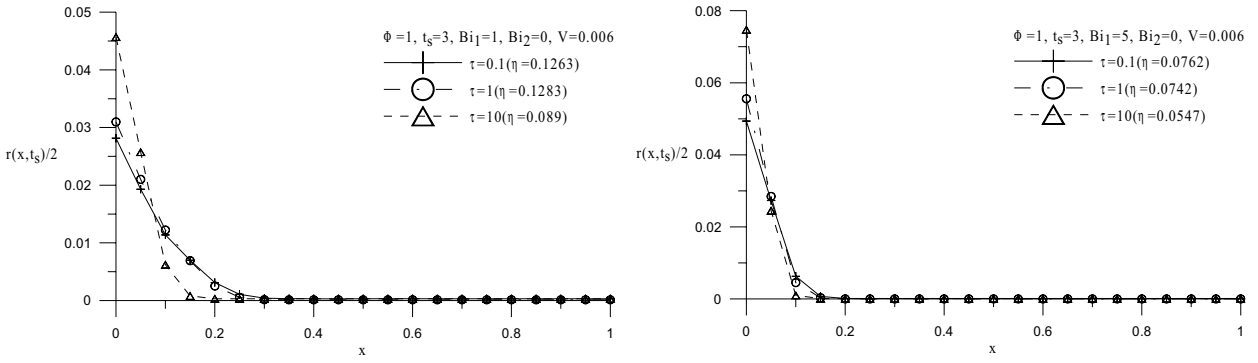

(a) (b)

Figure 8: The optimum longitudinal fin shapes at $t_s = 3$ and $V = 0.006$ by varying relaxation time τ and (a) $Bi_1 = 1$ and (b) $Bi_1 = 5$

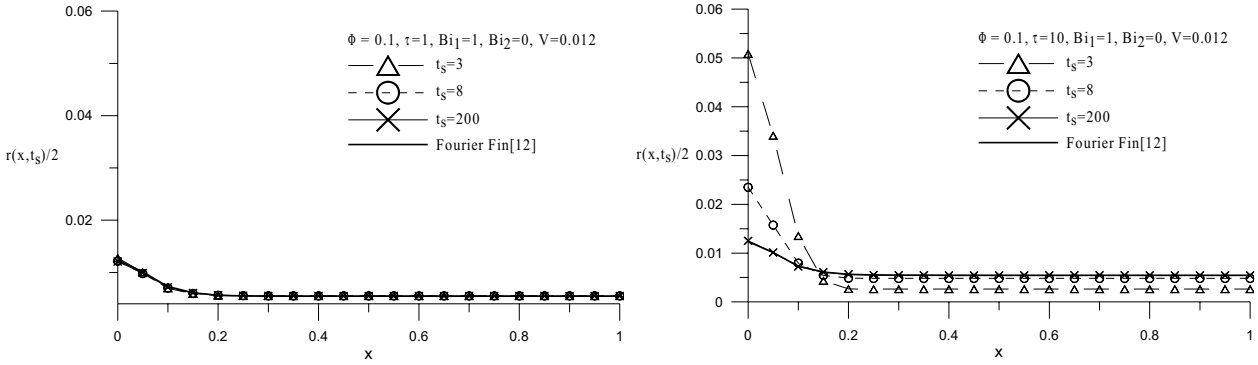

(a) (b)

Figure 9: The optimum longitudinal fin shapes at $\Phi = 0.1$ and $V = 0.012$ by varying t_s and (a) $\tau = 1$ and (b) $\tau = 10$

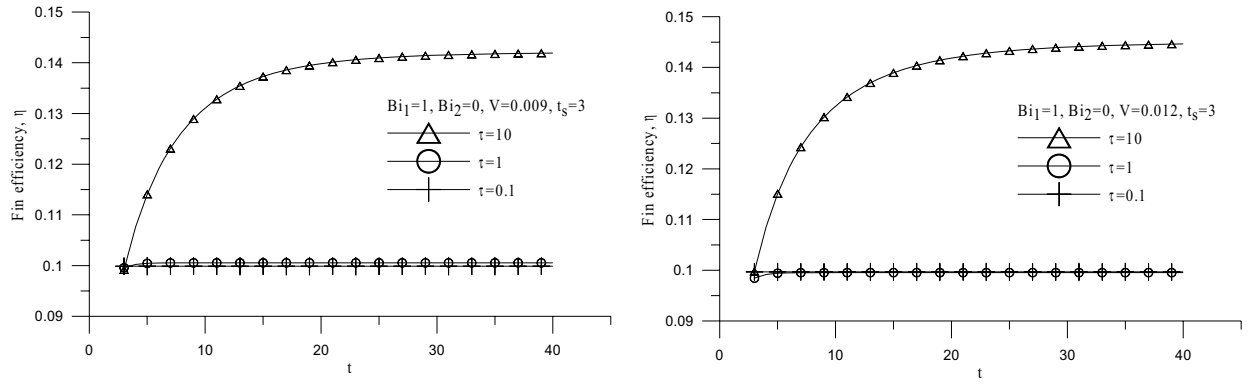

(a) (b)

Figure 10: The optimum longitudinal fin efficiency with time at $t_s = 3$ by varying relaxation time τ and (a) $V = 0.009$ and (b) $V = 0.012$

t_s increases and thus the fin profile is identical to the Fourier fin profile.

Finally the fin efficiency with time based on the optimum fin shape with desired fin efficiency $\Phi = 0.1$ obtained at $t_s = 3$ is examined for $V = 0.009$ and 0.012, respectively. The results are shown in Figures 10a and 10b for a comparison of the fin efficiency with time at different relaxation time and fin volume. It is clear that for the case $\tau = 0.1$ and 1, the fin reaches steady-state condition at $t_s = 3$ and thus the fin efficiency remains the same with time. However, for $\tau = 10$, the fin is still in a transient-state and the fin efficiency varies with time but will finally reach to a steady-state condition. Again, the fin efficiencies beyond $t_s = 3$ are all better than or equal to the efficiency at $t_s = 3$. This means the fin efficiency for the optimum fin is always better than or the same as the efficiency at $t_s = 3$ and therefore the overall fin performance is better than the desired value.

From the above discussions we concluded that the present design algorithm has the ability in designing optimum non-Fourier spine and longitudinal fins under the given constraints and the rate of convergence is also very fast.

9 Conclusions

The conjugate gradient method (CGM) was applied successfully for the solution of the inverse design problem in estimating the optimum shape of the non-Fourier spine and longitudinal fins. Several test cases involving different design considerations were examined.

It is noticed that when the Biot number varies, the optimum fin efficiency and optimum fin shape will be changed. The results also show that the fin efficiency can be improved greatly for the spine fins by the present design algorithm but can be increased only a little for the longitudinal fins. Moreover, the relaxation time plays an important role in the present optimum fin shape design problem. When it is small enough, the fin reaches to Fourier fin easily. When it becomes larger, the characteristic of the non-Fourier fin is dominated and the designed fin shape is different from the Fourier fin.

Acknowledgement: This work was supported in part through the National Science Council, R. O. C., Grant number, NSC-94-2611-E-006-021.

References

Alifanov, O. M. (1994): Inverse Heat Transfer Problems, Springer-Verlag, Berlin Heidelberg.

Aziz, A. (1992): Optimum Dimensions of Extended Surfaces Operating in a Convective Environment, *Applied Mechanics Review*, vol. 45, pp. 155-173.

Beck, J. V.; Blackwell, B.; St.Clairi, C.R. (1985): Inverse Heat Conduction Ill-Posed Problem, Wiley, New York.

Chao, R. M.; Chen, Y. J.; Lin, F. C. (2001): Determining the unknown traction of a cracked elastic body using the inverse technique with the dual boundary element method, *CMES-Computer Modeling in Engineering & Sciences*, vol. 2, pp. 73-85.

Chung, B. T. F. (1983): Chapter 21 Heat Transfer, ASM Handbook for Engineering Mathematics, American Society for Metals, Metal Park, OH.

Chung, B. T. F.; Iyer, J. R. (1993): Optimal Design of Longitudinal Rectangular Fins and Cylindrical Spines with Variable Heat Transfer Coefficient, *Heat Transfer Engng*, vol. 14, pp. 31-42.

Duffin, R. J. (1959): A Variational Problem Related to Cooling Fins, *J. Math. Mech.*, vol. 8, pp. 47-56.

Hon, Y. C.; Wei, T. (2005): The method of fundamental solution for solving multidimensional inverse heat conduction problems, *CMES-Computer Modeling in Engineering & Sciences*, vol. 7, pp. 119-132.

Huang, C. H.; Hsiao, J. H. (2003): An Inverse Design Problem in Determining the Optimum Shape of Spine and Longitudinal Fins, *Numerical Heat Transfer*, Part A, Vol. 43, pp. 155-177.

Huang, C. H.; Hsiao, J. H. (2003): A Non-linear Fin Design Problem in Determining the Optimum Shape of Spine and Longitudinal Fins, *Communications in Numerical Methods in Engineering*,

Vol. 19, No. 2, pp. 111-124.

Huang, C. H.; Hsiung, T. Y. (1999): An Inverse Design Problem of Estimating Optimal Shape of Cooling Passages in Turbine Blades, *Int. J. Heat and Mass Transfer*, vol. 42, pp. 4307-4319.

Huang, C. H.; Lo, H. C. (2006): A Three-Dimensional Inverse Problem in Estimating the Internal Heat Flux of Housing for High Speed Motors, *Applied Thermal Engineering*, vol. 26, No. 14-15, pp.1515–1529.

Huang, C. H.; Kim, S. (2005): An Inverse Problem for Estimating the Time-Dependent Reaction Coefficient in an Autocatalytic Reaction Pathway, *Chemical Engineering Science*, vol. 60, pp. 447-457.

Kern, D. Q.; Kraus, A. D. (1972): Extended Surface Heat Transfer, MacGraw-Hill, New York.

Kraus, A. D. (1988): Sixty-five Years of Extended Surface Technology (1922-1987), *Applied Mechanics Review*, vol. 41, pp. 321-364.

Lasdon, L. S.; Mitter, S. K.; Warren, A. D. (1967): The Conjugate Gradient Method for Optimal Control Problem, *IEEE Transactions on Automatic Control*, AC-12, pp. 132-138.

Lin, J. Y. (1998): The non-Fourier effect on the fin performance under periodic thermal conditions, *Appl. Math. Model*, vol. 22, pp. 629–640.

Liu, C. S. (2006): An efficient simultaneous estimation of temperature-dependent thermophysical properties, *CMES-Computer Modeling in Engineering & Sciences*, vol. 14, pp. 77-90.

Liu, C. S.; Liu, L. W.; Hong, H. K. (2007): Highly accurate computation of spatial-dependent heat conductivity and heat capacity in inverse thermal problem, *CMES-Computer Modeling in Engineering & Sciences*, vol. 17, pp. 1-18 .

Razelos, P. (1983): On Optimum Dimensions of Convective Pin Fins, *J. Heat Transfer*, vol. 105, pp. 411-413.

Schmidt, E. (1926): Die Warmeubertragung durch Rippen, *Z. VDI*, vol. 70, pp. 885-947.

Wilkins, J. E. Jr. (1960): Minimizing the Mass of Thin Radiating Fins, *J. Aerospace Sci.*, vol. 27, pp. 145.

Wilkins, J. E. Jr. (1960): Minimum Mass Thin Fins with Transfer Heat only by Radiation to Surrounding at Absolute Zero, *J. Soc, Ind, Appl, Math.*, vol. 8, pp. 630-639.

Yeh, R. H. (1996): Optimum Dimensions of Longitudinal Rectangular Fins and Cylindrical Pin Fins with Variable Heat Transfer Coefficient, *The Canadian J. of Chemical Engineering*, vol. 74, pp. 144-151.